On-Substrate Preparation of an Electroactive Conjugated Polyazomethine from Solution-Processable Monomers and its Application in Electrochromic Devices

*Lambert Sicard, Daminda Navarathne, Thomas Skalski, and W. G. Skene**

An electroactive polyazomethine is prepared from a solution processable 2,5-diaminothiophene derivative and 4,4′-triphenylamine dialdehyde by spray-coating the monomers on substrates, including indium tin oxide (ITO) coated glass and native glass slides. The conjugated polymer was rapidly formed in situ by heating the substrates at 120 °C for 30 min in an acid saturated atmosphere. The resulting immobilized polymer is easily purified by rinsing the substrate with dichloromethane. The on-substrate polymerization is tolerant towards large stoichiometry imbalances of the comonomers, unlike solution step-growth polymerization. The resulting polyazomethine is electroactive and it can be switched reversibly between its neutral and oxidized states both electrochemically and chemically without degradation. A transmissive electrochromic device is fabricated from the immobilized polyazomethine on an ITO electrode. The resulting device is successfully cycled between its oxidized (dark blue) and neutral (cyan/light green) states with applied biases of +3.2 and −1.5 V under ambient conditions without significant color fatigue or polymer degradation. The coloration efficiency of the oxidized state at 690 nm is 102 cm^2 C^{-1}.

1. Introduction

Conjugated organic polymers have many interesting optoelectronic properties that are well suitable for their use in plastic electronics including field effect transistors, photovoltaic, light-emitting, and electrochromic devices.[1] Well-developed synthetic methods have provided the means to prepare solution processable conjugated polymers having desired optoelectronic properties.[1b,2] While solution processability of the polymers is required for straightforward device fabrication and accurate polymer characterization, in some instances this feature can be problematic. This is especially true for electrochromic applications.[3] A solution processable polymer, when used as the electroactive layer in electrochromic devices, is often miscible with the electrolyte gel.[3c,3d] This is problematic because the electroactive layer subsequently delaminates from the electrode resulting in limited device lifetime, poor device performance, localized color defects, and poor color contrast.

Many approaches have been developed to address these shortcomings, notably changing the polymer solubility with cleavable groups that are incorporated into the polymer. These reactive groups can be released using external triggers such as heat, catalysts, or light after depositing the solution processable polymers on the substrate.[3d,4] While this approach is an effective means of immobilizing polymers on the substrate for preventing their mixing with the different device layers, the preparation of these convertible polymers requires additional and challenging synthetic efforts. Alternatively, electroactive monomers can be immobilized on the electrode by electropolymerization either ex situ or in situ.[5] This requires the monomers to have low oxidation potentials for minimizing the risk of producing over oxidized by-products and other undesired defects. Moreover, α-β coupling defects must be avoided to ensure desired optoelectronic properties are obtained. Preparing monomers that satisfy these extensive criteria are not only complex, but the reactive monomers are susceptible to spontaneous anodic polymerization under ambient conditions. This often leads to variable products and inconsistent opto-electronic properties.[6] Simpler means of obtaining immobilized conjugated polymers in a controlled manner that are stable under ambient conditions without sacrificing the opto-electronic properties are therefore of interest.

Azomethines are suitable materials that address the stringent immobilization criteria. This is in part owing to their preparation that involves simple dehydration in bulk and that does not require stringent reaction conditions or catalysts. The complementary reactivity of the amine and aldehyde monomers additionally ensures the exclusive azomethine formation without undesired side reactions or defects, in contrast to their anodically prepared counterparts. Conjugated polyazomethines are further known to be poorly soluble in common device preparation solvents, which is a desired trait for resisting delamination from the electrode with the electrolytic gel.[7] Azomethines also

L. Sicard,[+] Dr. D. Navarathne, T. Skalski,
Prof. W. G. Skene
Laboratoire de caractérisation photophysique
des matériaux conjugués
Département de chimie
Université de Montréal
CP 6128, Centre-ville, Montreal, QC
E-mail: w.skene@umontreal.ca
[+]Present address: Laboratoire de Chimie des Polymères - UMR 7610, Université Pierre et Marie CURIE (Paris 6), Site St Raphaël, 3 rue Galilée, 94200 Ivry-sur-Seine, France

DOI: 10.1002/adfm.201203657

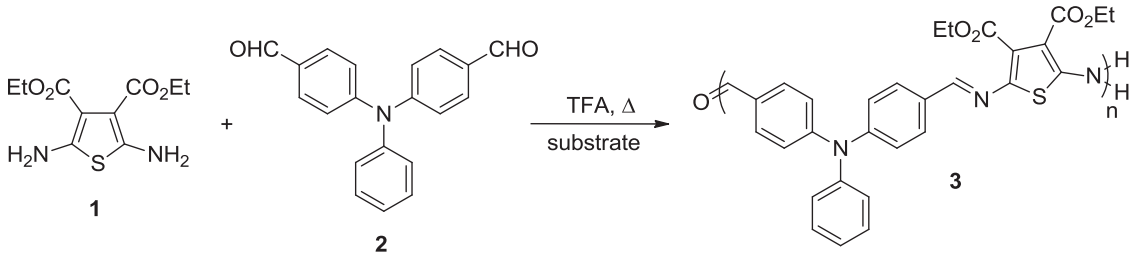

Scheme 1. On-substrate polymerization of the electroactive polyazomethine **3**.

benefit from an inherent electron withdrawing character. When prepared from electron donating monomers, the resulting materials have an alternating electron donor-acceptor configuration. Such electronic push–pull systems are highly conjugated and they absorb boldly in the visible.[8] Their discrete absorbances can additionally be tuned across the entire visible spectrum contingent on the degree of conjugation and the precursors used for their preparation, while having the advantage of being easy to prepare.[8a,9] This is in contrast to their counterparts prepared by conventional aryl–aryl coupling protocols that require extensive synthetic and purification protocols.[4f,10] The most important polyazomethine properties desired for using these conjugated polymers in electrochromic devices is reversible oxidation, vibrant color change between their neutral and charged states, along with the stability of both the neutral and oxidized states under ambient conditions.[8b,11]

Despite their optoelectronic properties that are well suited for use in electrochromic applications, polyazomethines have not been successfully used as electrochromic layers in devices.[9b,12] Additionally, conjugated polyazomethines have not been prepared directly on the electrode surfaces to afford immobilized polymers. Herein, we report the straightforward de novo preparation of conjugated polyazomethines via an on-substrate polymerization method using solution-processable monomers deposited directly onto ITO or glass surfaces. Electrochemical, spectroelectrochemical and switching studies of the on-substrate prepared polyazomethine are also discussed. An electrochromic device capable of switching between colored states under ambient conditions is further demonstrated. This represents the first successful example of a working electrochromic device using a polyazomethine as the electrochromic layer in addition to the on-substrate polymerization of the electroactive polymer.

2. Results and Discussion

2.1. On-substrate Polymerization

Polyazomethines have been extensively studied with phenyldiamine.[12b,12c,16] However, **1** (**Scheme 1**) is a more suitable monomer for preparing polyazomethines for electrochromic applications. This is in part because it yields conjugated azomethines that absorb intensely in the visible portion of the spectrum. Moreover, their oxidized states are also intensely colored. This results in a large color change between the neutral and charged states, which is a desired property for electrochromic applications. The triarylamine monomer **2** was chosen as a complementary monomer for condensing with **1**. This was because the resulting polyazomethine (**3**) was expected to absorb more in the yellow region of the spectrum than its all-thiophene polyazomethine counterpart.[17] This is a result of large twist angles between the homoaryl moieties and the azomethines of **3** that limit its degree of conjugation. However, its charged state was expected to be significantly colored because of intramolecular charge transfer courtesy of the electron rich triarylamine.[18] A bold color transition between the neutral and charged states was therefore expected for the electroactive **3**, resulting in a electrochromic material whose switching could easily be seen by the eye. This is a desired property for use in low-resolution and large area electrochromic display applications such as signs and billboards.

The on-substrate polymerization of **3** was initially done using stoichiometric amounts of the complementary comonomers. These conditions were used because step-growth polymerization is known to be intolerant towards comonomer stoichiometric imbalances.[19] Only trimers and lower molecular weight oligomers are obtained when the molar ratio of the comonomers is varied by more than 1 mol%. The 1:1 mole ratio of **1** to **2** was further used to test the polymerization conditions required to produce **3**. Since this ratio was expected to yield **3**, the effect of the monomer concentration on the resulting comonomer and polymer films deposited on the substrate could also be examined.

The polymerization of **3** was done by spray-coating the premixed comonomer solutions onto glass substrates. The substrates were then heated between 60 and 150 °C in a TFA saturated environment. TFA was chosen as the catalyst because of its high vapor pressure. A saturated acid atmosphere at low temperatures is therefore possible. It is also a strong acid capable of catalyzing azomethine formation in the solid state.[20] The optimum temperature for the polymerization was 120 °C. This ensured evaporation of the water by-product, shifting the azomethine equilibrium towards formation of the polymer. A polyazomethine film that was insoluble in dichloromethane was obtained after 30 min of polymerization. This is in contrast to the polymerization of conjugated polyazomethines in solution that requires up to 48 h for obtaining high yields of high molecular weight polymers.[21] Increased reaction times of 90 min did not alter the polyazomethine film or its absorbance spectrum.

As desired, the resulting film of **3** was strongly physisorbed onto the substrate and it could not be removed with soxhlet extraction using dichloromethane and THF. The insolubility of the resulting polymers precluded its characterization by conventional solution based polymer identification techniques. Polyazomethine formation could nonetheless be spectroscopically

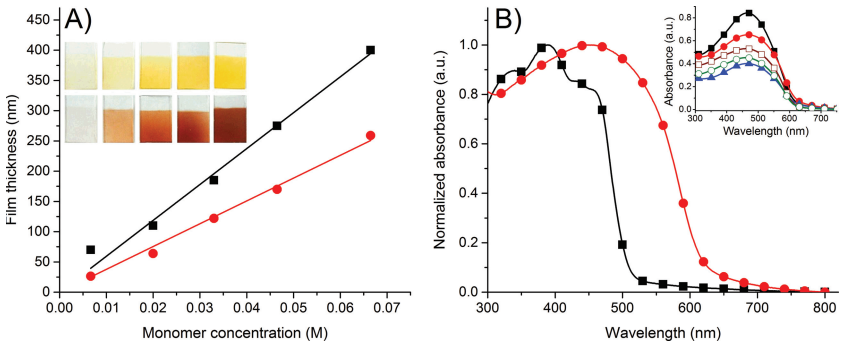

Figure 1. A) Correlation of monomer concentration and film thickness determined by stylus profilometry before (■) and after (●) polymerization of spray-coated films with a 1:1 stoichiometry of monomers **1** and **2**. Inset: photographs of the corresponding spray-coated films before (top) and after (bottom) polymerization of 1.86, 5.58, 9.30, 13.0, and 18.6 mg/mL solutions of comonomers (from left to right). B) Normalized absorbance spectra of a 1:1 stoichiometry mixture of monomers **1** and **2** spray-coated onto a glass substrate measured before (■) and after (●) polymerization. Inset: absorbance spectra of the polymerized films of **3** as a function of mole ratios of **1** and **2**: 2:1 (▲), 1.5:1 (□), 1:1 (■), 1:1.5 (●), and 1:2 (○).

assessed owing to its increased degree of conjugation relative to its precursors. As seen in the inset of **Figure 1**A, the spray-coated monomer films changed from their initial yellow to a red brown color upon polymerization. The color change is further supported spectroscopically via the absorbance spectra as per Figure 1B. Since TFA can potentially protonate the azomethine and it could be responsible for the observed color change, the resulting polymer films were therefore rinsed with copious amounts of a triethylamine solution.[21c] The organic base is known to readily deprotonate the protonated azomethine, resulting in the neutral imine bond.[12a] The substrates were also rinsed with abundant amounts of dichloromethane to ensure the removal of any unreacted comonomers and lower molecular weight oligomers. No color change was observed with the polymer film with such rinsing. Figure 1B shows the absorbance spectra of the spray-coated film before (black line) and after (red line) the polymerization. The before polymerization film had a relatively narrow absorbance peak with a maximum absorbance of 390 nm and an onset of 514 nm. Whereas, the film after polymerization had a broader and red-shifted absorbance with a maximum of 460 nm and an onset of 612 nm. The peak broadening as well as the red-shifted absorbance concomitant with the insoluble film collectively provide resounding evidence for the polymerization of polydisperse **3** on the substrate.

The inset of Figure 1A shows photographs of a series of polymer films on glass slides obtained by spray-coating various concentrations of comonomer solutions of equal mole ratios. The pictures in the top row are of the films before the polymerization while the bottom row shows the corresponding films after the TFA catalyzed on-substrate polymerization. It is evident that the film thickness can be tailored between 50 and 400 nm by adjusting the monomer concentration. The films after polymerization were found to be ca. 40% thinner (vide infra) compared to the as spray-coated monomers. Nonetheless, the linear trend seen in Figure 1A confirms that the thickness of the films can be tailored. Moreover, the thickness of the polymer layer of **3** can be tuned between 20 and 250 nm as a function of the comonomer concentration.

Atomic force microscopy measurements were done to confirm polymer coverage of the substrate with the on-substrate polymerization method. These measurements were also done for qualitatively examining the polymerization induced morphological changes to the films. Monomer spray-coating was preferred over spin-coating because thicker films of **3** were possible, resulting in desired pronounced color transitions that were visible to the eye. However, AFM measurements were done with polymer films prepared from spin-coated monomers. This deposition method was preferred in order to minimize the artifacts including inhomogeneous and variably thick films possible by uneven spray-coating techniques. The thinner films obtained by spin-coating are also advantageous for confirming polymer formation. **Figure 2** shows the AFM micrographs of the films obtained before and after the polymerization as well as the film cross sections. These AFM images reveal that the film prior to the polymerization had a lower average roughness value (R_a) as compared to the film after the polymerization. While the AFM micrograms serve exclusively to qualitatively assess the films, they nonetheless confirm that a polymer film covers the entire substrate. This is of importance because minimal diffusion in the solid state could potentially prevent polymerization and result in limited imine formation. Removing the ensuing soluble oligomers and unreacted monomers with rinsing would lead to localized regions where the film would be stripped to the bare substrate upon washing. This would lead to extremely rough surfaces with detectable pits in the polymer layer. In contrast, the AFM measurements confirmed that the resulting polymerized film was consistently thick with no detectable areas of exposed substrate from pitting. This confirmed that the polymerization of the deposited monomer is not confined to localized areas, but that it propagates across the entire substrate both vertically and laterally.

The absolute thickness of the pre- and polymerized films could not be measured using an AFM scratch method owing to the large thicknesses of the spray-coated films.[22] The desired film heights were therefore measured by stylus profilometry. It was found that the polymerized film decreased 37% on average relative to the monomer spray-coated film thickness. The decrease in the film thickness and the change to the film morphology with polymerization can be attributed to removal of the unreacted comonomers and low molecular oligomers with dichloromethane washings. Meanwhile, the consistently and homogeneously thick post-reaction film that resists rinsing with dichloromethane further corroborates that the resulting film is a polymer.

The polymerization of **3** follows a step-growth mechanism that usually requires a strict control of the stoichiometry between the comonomers when done in solution. However, it was observed that the on-substrate polymerization was tolerant towards imbalances in the comonomer mole ratio. This was confirmed by examining the effect of different mole ratios of **1** and **2** on the absorbance at 470 nm for the polymer **3** obtained.

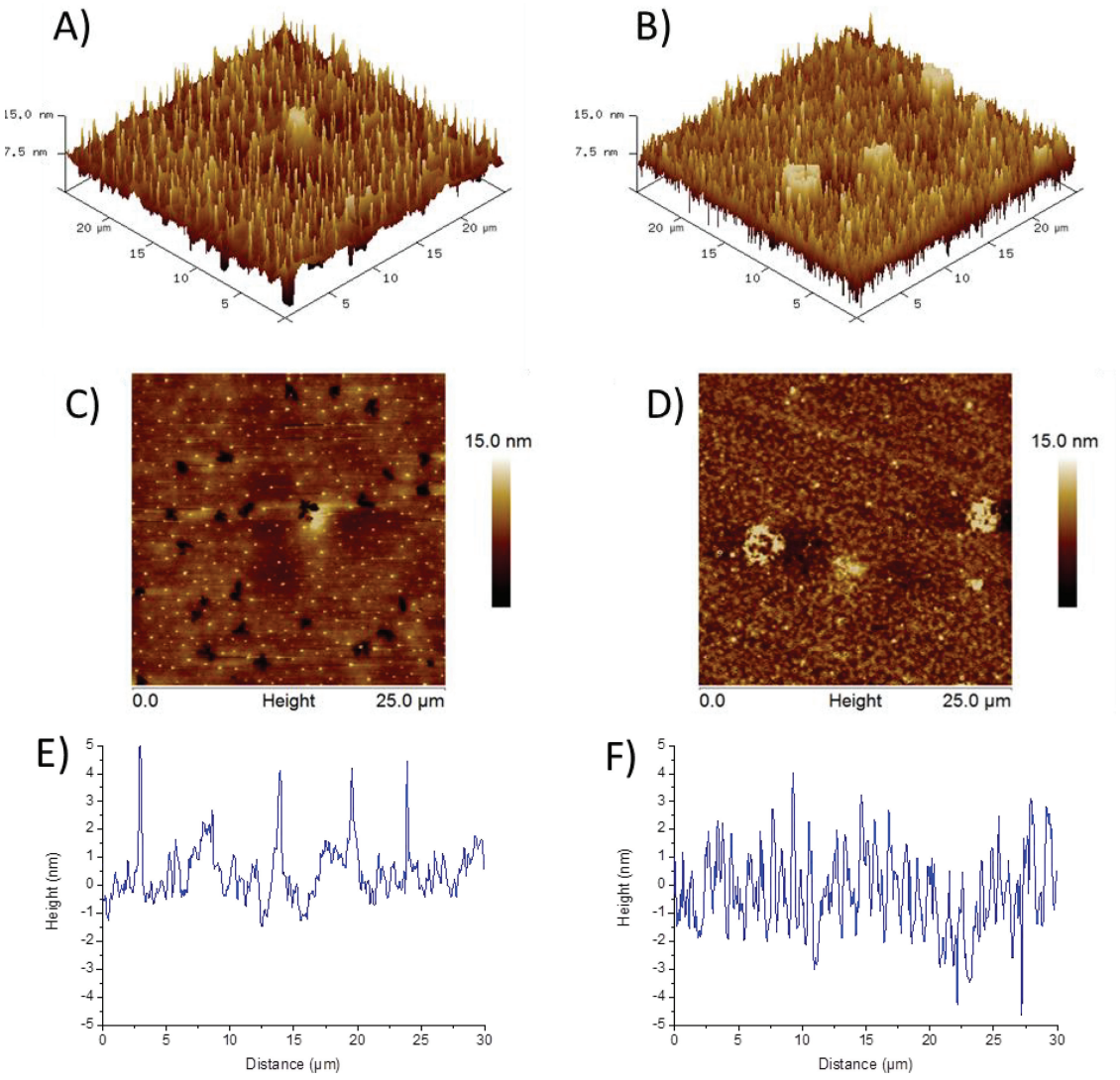

Figure 2. AFM tapping micrographs of films of spin-coated monomers **1** and **2** on A,C) glass substrates and the B,D) resulting **3** obtained by on-substrate polymerization. AFM cross section micrographs E) before and F) after polymerization. Respective average roughness (R_a) values are 0.750 and 1.16 nm.

This wavelength was chosen as a suitable metric for assessing the polymer because the λ_{max} is sensitive to variations in the degree of polymerization.[23] **Table 1** shows a series of films of **3** obtained on glass substrates by spray-coating various molar ratios of the two monomers and their corresponding polymer films. In all cases, the total monomer concentration of the mixture remained constant. It was possible to obtain polymer films that were immobilized on the substrate even with large variations in mole ratios of the two comonomers, i.e., 1:2 and 2:1 ratio of **1**:**2**. This is in contrast to the solution polymerization that affords uniquely trimers with these conditions. These trimers and other low molecular weight oligomers are extremely soluble in the solvents that were used to wash the polymerized surfaces of **3**. Therefore, they would be removed from the surface.[24] The collective results confirm that a polymer is formed by the on-substrate method even when exact stoichiometric ratios of the comonomers are not used. Rather, varying the comonomer ratio affects the thickness of the polymer film. The thickest films were obtained with stoichiometric amounts of **1** and **2**. As seen in the absorbance spectra in Figure 1B and the photographs of the films in Table 1, only the intensity of the

Table 1. Photographs of polymer films of **3** as a function of different comonomer mole ratios and their optical energy-gaps.

Photographs of the films	a)	b)	c)	d)	e)
Mole ratio of **1**:**2**	2:1	1.5:1	1:1	1:1.5	1:2
2 [mg/mL]	6.6	6.0	5.0	4.0	3.6
1 [mg/mL]	3.1	3.4	4.3	5.1	5.7
Total concentration [mol/mL]			3.3×10^{-5}		
Optical energy-gap [eV][f)]	2.03	2.03	2.02	2.01	2.01

[a–e)]Mole ratio of **1**:**2** as per the first row of the table. [f)]Taken from the absorbance onset.

film changes when [1] ≠ [2]. The observed decrease in the absorbance intensity is a result a reduced thickness of the polymer film. According to the consistent λ_{max} and the optical energy-gaps, all the polymers obtained by the on-substrate method have comparable conjugation lengths despite their mismatched comonomer stoichiometries. The consistent λ_{max} further suggests that the polymers have a minimum average degree of polymerization (DP) of 10. This is according to similar polyazomethines whose absorbance shifts did not undergo additional bathochromic shifts with DP ≥ 10.[21b] It should be noted that extended bathochromic shifts for the polymer's absorbance are not expected. This is a result of twisting of the mean planes between the azomethine and triaryl amine that limits their degree of conjugation.[25] This is in contrast to heterocyclic azomethines that are red-shifted owing to their high degree of coplanarity that promotes extensive delocalization.[8,26] The twisting of **3** is expected to separate the polymer chains into a series of chromophores. This is beneficial for color reproducibility unlike fully conjugated polymers whose optical properties are affected by polymer conformation.[27]

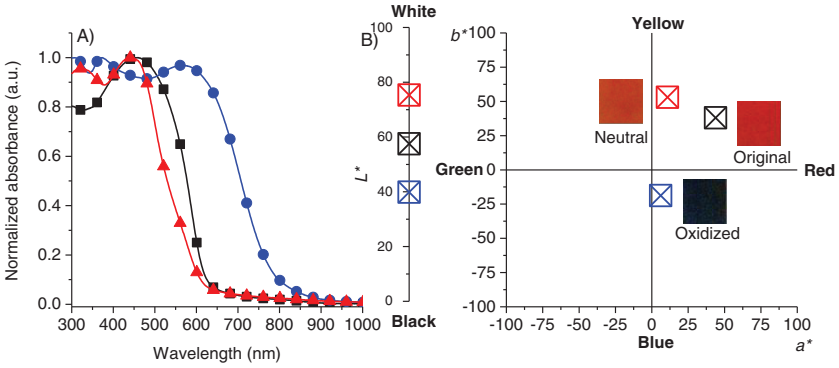

Figure 3. A) Normalized absorbance spectra of films of **3** on glass substrates measured in their neutral state (■), chemically oxidized with $FeCl_3$ (●), and subsequent neutralization with hydrazine hydrate (▲). B) The corresponding CIE D65 color coordinates and photographs of the various states of **3** from (A).

2.2. Color Changes of Charged States

Both reversible oxidation and detectable color change between the polymer's neutral and charged states are paramount for using the material in electrochromic applications. Thus, the reversible oxidation of **3** and its color change were examined both chemically and electrochemically. The neutral state of the immobilized **3** on glass substrates was red (460 nm) as seen in **Figure 3**A. Its color turned to blue (580 nm) when oxidized by immersing the substrate in a 0.1 M dichloromethane solution of $FeCl_3$ that was used as the oxidant. The corresponding CIE $L^*a^*b^*$ color coordinates and photographs of the different states are shown in Figure 3B and Table 1. The blue color persisted and it did not fade when removing the substrate from the solution. Color dissipation would otherwise indicate degradation/hydrolysis of the polymer and instability of the oxidized state. The polymer could be neutralized by immersing the substrate in a dichloromethane solution containing hydrazine. This quenched the blue color giving rise to an orange (450 nm) film. Switching between the orange and blue colored states of the polymer film was possible by subjecting the substrate to multiple oxidation/neutralization cycles with ferric chloride and hydrazine hydrate, respectively. The successive washing cycles led to no significant color degradation or variation in the absorbance intensity. No special precautions were also required for handling the material in its different states, illustrating its air stability. These behaviors demonstrate the robustness of the film and the azomethine bonds towards chemical doping. Furthermore, the reversibility of the doping process under ambient conditions implies that both the neutral and the oxidized states are stable.

The reversible electrochemistry of **3** was further investigated by cyclic voltammetry. For this, the polymer was subsequently prepared on transparent ITO electrodes using the on-substrate polymerization method. The cyclic voltammogram (CV) depicted in **Figure 4**A was obtained in a tetrabutyl ammonium hexafluorophosphate ($TBAPF_6$) solution of acetonitrile and **3** was immobilized on an ITO-electrode that served as the working electrode. A platinum wire counter electrode and

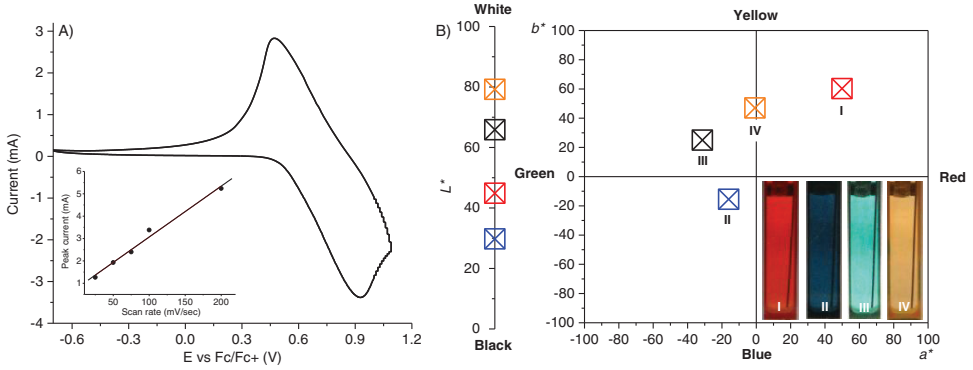

Figure 4. A) Cyclic voltammogram of the immobilized film of **3** on an ITO-coated glass electrode measured in 0.1 M $TBAPF_6$ in acetonitrile at a scan rate of 100 mV/s. Inset: peak current as a function of scan rate of **3** immobilized on ITO. B) Inset: photographs (from left to right) of the immobilized film of **3** on ITO-coated glass electrode in its original (I), oxidized (II) neutral and oxidation (III), and reduced (IV) states and the corresponding CIE D65 coordinates.

Ag/Ag^+ non-aqueous reference electrode were also used. From the cyclic voltammogram showing the anodic scan (Figure 4A), it is evident that the oxidation process of **3** at 700 mV is reversible. This is in contrast to its corresponding dimers and trimers that are irreversible oxidized.[24] The reversible oxidation confirms that the polymer is anodically stable at ambient conditions and that the electrochemically generated intermediate is also stable, a required property for use in electrochromic devices. **3** is interestingly the first example of a non-metal coordinated polyazomethine that can be reversibly oxidized. However, the electrochemically generated intermediate cannot be unequivocally assigned from the peak separation according to standard means.[28] The intermediate is nonetheless assumed to be a radical cation. Meanwhile, the broad E_{pc}/E_{pa} separation is consistent with a polymer having multiple oxidation sites.[29] The change in peak current with scan rate was additionally investigated. This was done to confirm that the electrochemical process measured was from the polymer immobilized on the electrode and not from material desorbing into solution from the substrate. The linear correlation of peak current as a function of scan rate observed in the inset of Figure 4A is consistent with physisorbed electroactive materials on the electrode. This confirms that the polyazomethine is robustly immobilized on the electrode, as desired. The robust immobilization was further supported visually, where no running of the color from the substrate into the electrolyte solution was observed with repeated cycling between the neutral and oxidized states.

The spectroelectrochemistry of **3** immobilized on the working ITO electrode was also investigated. This was done in part to assess the color transition and switching capacity of the polymer under conditions similar to those in a working electrochromic device. The spectroelectrochemistry of **3** was also done to corroborate the chemical doping studies. For the spectroelectrochemical studies, the oxidation potential, oxidation reversibility, color changes, and the oxidation/neutralization switching rates of the immobilized polymer were investigated in acetonitrile using $TBAPF_6$ as the supporting electrolyte and by applying a bias of + 1.1 and –0.7 V vs. Fc/Fc^+. The electrochemical oxidation of **3** led to stark color changes between its neutral and oxidized states. In contrast to the chemical doping studies, four distinct color states; red (**I**), deep blue (**II**), cyan (**III**) and orange (**IV**), were observed by spectroelectrochemistry. The oxidation of **3** at 1.1 V resulted in a deep blue color corresponding to its oxidized state (**II**). An applied bias of –0.7 V resulted in the neutral state (**III**) whose color was cyan. The polymer could be repeatedly switched (vide infra) between its two colors, corresponding to the oxidized (**II**) and neutral (**III**) states, with positive and negative biases, respectively. However, the original color of state **I** could not be obtained even at large negative potentials. Instead, applying a large negative potential of –1.9 V led to an orange colored reduced state (**IV**). The reduced polymer could be switched sequentially to states **III** and **II**, but the resulting states were less intense than those observed before applying the –1.9 V potential. The large negative potential had to be applied for extended times in order to obtain state **IV**. These harsh conditions eventually destroyed the polymer's electroactivity (see the Supporting Information), resulting in the reduction of the azomethines bonds. Meanwhile, the color difference between the neutral states obtained after electrochemical and chemical oxidation is a result of the different counter ions that are trapped in the polymer film and that remain complexed with the polymer after the first oxidation cycle.

Table 2. CIE coordinates with D65 illuminant and 2° observer angle for the different states of **3**.

	State	L*	a*	b*
Chemical doping[a)]	Oxidized	40	6	–19
	Neutral	75	11	53
Solution[b)]	I	45	49	60
	II	29	–16	–15
	III	66	–31	25
	IV	79	–0.8	47
Device[c)]	Oxidized	62	–15	–19
	Neutralized	86	–20	14

[a)]**3** immobilized on glass substrates and coordinates measured upon oxidation and neutralization with ferric chloride and hydrazine hydrate, respectively, in dichloromethane; [b)]**3** immobilized on the ITO electrode and coordinates measured at the equilibrium state electrochemically in acetonitrile with $TBAPF_6$ as the supporting electrolyte; [c)]**3** measured when it was used as the electrochromic layer in the working transmissive electrochromic device.

The CIE coordinates of the different states obtained with D65 illuminant and 2° observer angle are summarized in **Table 2**. Meanwhile, the colors of the various electrochemically produced states are seen in the photographs of Figure 4B. It is noteworthy that the electrochemical switching was done under ambient conditions without deaerated or anhydrous solvents, demonstrating the stability of both the neutral and oxidized states. The collective chemical and electrochemical studies demonstrate that **3** has spectral and electrochemical properties that are suitable for its use as the electrochromic layer in devices. **3** is further interesting because it is the first example of a polyazomethine that can be reversibly oxidized and it exhibits significant color changes in the visible spectrum between its neutral and oxidized states.

The switching speed and duty cycle of the immobilized polymer were additionally investigated to further asses the stability and robustness of the electrochromic material. The duty cycle of the immobilized polymer was examined with 5 s switching speeds. This switching interval was chosen because it was found to give the highest percent transmittance change between the neutral and oxidized states. As seen in **Figure 5**A, the polymer could be switched up to 150 cycles without any significant variation in the transmittance. The upwards drift in the transmission variation observed at extended switching times is due to drifting in the lamp intensity and not from polymer degradation or charge storage. These would otherwise be observed as a decrease in the absolute transmission difference between the oxidized and neutral states instead of the consistent absolute transmission difference observed with switching. **3** could also be switched between its two colored states at various speeds as seen in Figure 5B. Fast switching speeds up to 0.2 s were possible. However, the transmittance difference decreased from 34 to 3% with increasing switching speeds from 30 to 0.2 s. The optimal switching time was found to be 5 s, determined from the consistent maximum transmission difference derived from

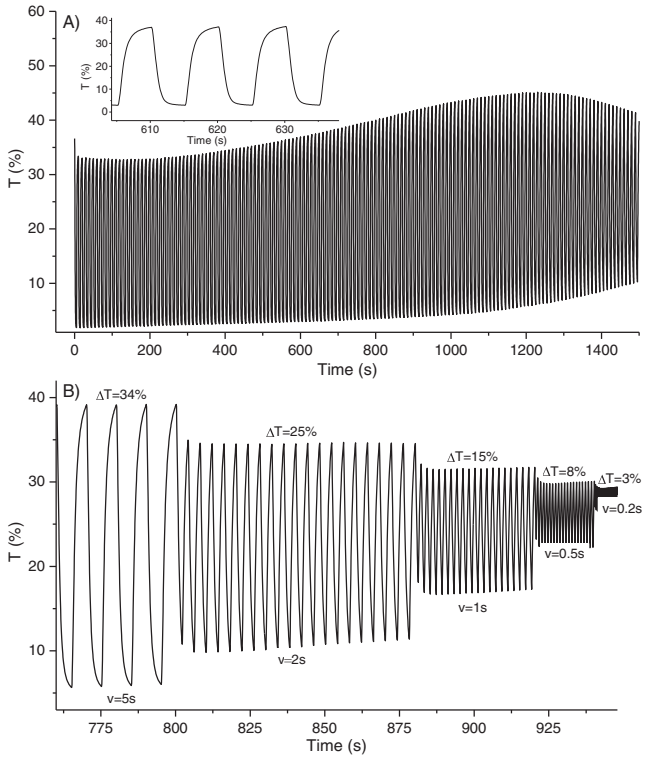

Figure 5. A) Duty cycle of **3** immobilized on an ITO electrode and measured in acetonitrile with $TBAPF_6$ as the electrolyte. The bias was switched between +1.1 and −0.7 V vs. Fc/Fc^+ at 5 s intervals and the transmission was monitored at 694 nm. Inset: expansion showing the change in transmittance at 694 nm for three complete switching cycles at 5 s intervals. B) Change in transmittance of **3** immobilized on an ITO electrode similar to (A) as a function of different switching speed.

the switching speeds. The decrease in transmittance difference with increasing switching speed is a result of slow diffusion of the bulky $TBAPF_6$ electrolyte through the polymer film. The collective spectroelectrochemical data confirm that **3** is robust and that it can withstand repeated switching between its neutral and oxidation state under ambient conditions. The film could also be switched again between its different states even after extended rest periods under ambient conditions without significant decrease in the absolute transmission difference. While extended duty cycles are ultimately beneficial for end-user applications, the switching cycles observed in Figure 5A are nonetheless the first example of an azomethine polymer capable of such repeated cycling without color fatigue or decomposition. Extended duty cycles comparable to aryl-aryl type materials are expected with **3** with improved film preparation, controlled film thickness, and different electrolytes.

2.3. Electrochromic Device

In light of the electrochemically induced reversible color states of the immobilized polymeric film of **3** on ITO substrates observed in solution, a transmissive window type electrochromic device was fabricated from the polyazomethine. This was done using the on-substrate method by polymerizing **3** directly on the ITO electrode, similar to the solution studies. Two sets of devices with **3** were prepared using the standard ITO/electrochromic layer/electrolytic gel/ITO electrochromic device architecture.[5b,15] No defined counter electrode material was used in this simplified device architecture. One device was prepared by covering completely the ITO electrode with spray-coated monomers. Another device was prepared by selectively depositing monomers onto the electrode by spraying them over a stencil mask. The pattern of the spray-coated monomers on the electrode was preserved without visual degradation or blurring of the image with the formation of **3**. Prior to assembling the device, the electrode with the immobilized **3** was immersed in an acetonitrile solution with $TBAPF_6$. The film was then subjected to a couple of oxidation/neutralization cycles until a consistent cyan to green color transition was achieved. Devices fabricated without this pre-switching step resulted in different colors than devices prepared with the pre-switching step. The color inhomogeneity is ascribed to physisorbed oligomers and unconverted monomers that migrate to the film-solution interface with oxidation/neutralization cycles, where they subsequently diffuse into the bulk solution. The oxidation/neutralization pre-device fabrication treatment electrochemically purifies the polymer film by removing the residual low molecular weight products that are not removed with alkaline rinsing. Electrochromic devices were fabricated by sandwiching a UV curable gel electrolyte between a blank ITO electrode and an ITO-covered **3** by using a double sided black foam tape as a spacer. It was found that **3** was robustly immobilized on the electrode given that it did not delaminate from the substrate during the device assembly. The device was subsequently fabricated in an easy and straightforward fashion. This is in contrast to oligomeric azomethines that either decompose or delaminate from the electrode and mix with the electrolyte gel under similar conditions. These challenges have limited the success of previously investigated materials for electrochromic materials.

Devices consisting of **3** as the electrochromic layer were tested using a bias of +3.2 and −1.5 V. The resulting device color changes observed with these potentials are shown in the photographs in the top panel of **Figure 6**. These show the electrochromic film in its original (left), oxidized (right) and neutral states (middle). The devices were vibrant cyan/green and dark blue for the neutral and oxidized states, respectively. It is evident from the photographs that the colors of both the neutral and oxidized states of the device are comparable to the colors observed electrochemically with the immobilized **3** on the ITO electrode in solution (Figure 4B). The similarity of the original neutral and oxidized colored states was further confirmed quantitatively via the CIE color coordinates that are shown in Figures 4B and 6B in addition to Table 2. At first glance, the colors of the neutral state after oxidation for both the device (green, Figure 6) and the immobilized **3** on ITO in solution (teal, Figure 4B) appear different. However, the CIE color coordinates in Table 2 are similar for the two states and the absorbance spectra of Figures 6A and Supporting Information Figure S1 are also identical. The perceived color difference is a result of a slight increase in the absorbance at 668 nm for the neutral state in the working device. This adds a minute red component to the color that is perceived as teal instead of green.

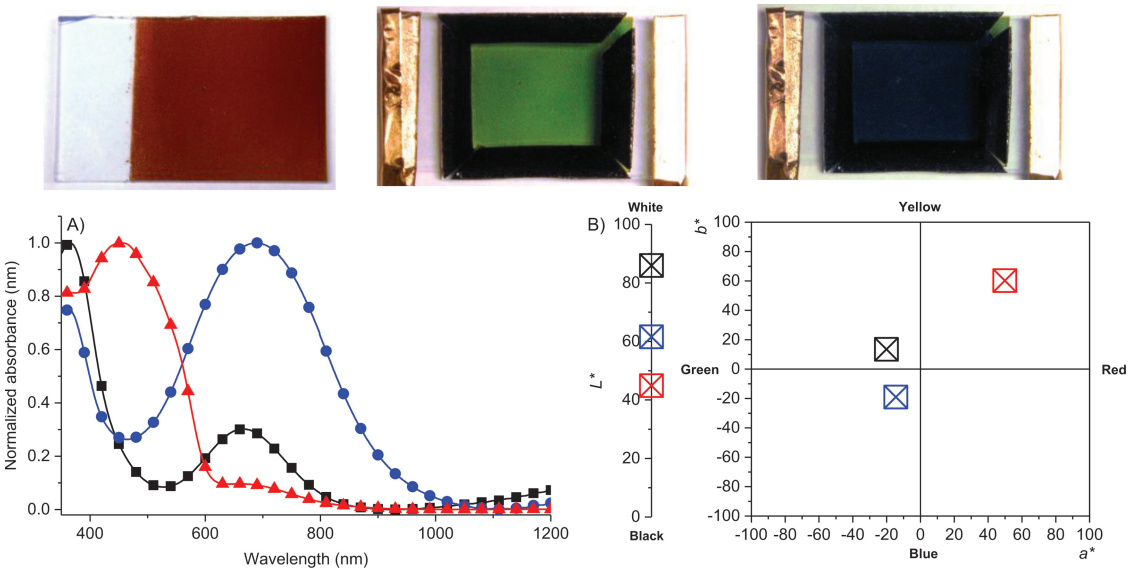

Figure 6. Top panel: photographs of the on-substrate polymerized film of **3** (left), the corresponding electrochromic device upon oxidation (right) and the neutral state after an oxidation cycle (middle). A) Normalized absorbance spectra of the on-substrate polymerized film of **3** (▲), the corresponding electrochromic device in its oxidized state (●) and the neutral state after a complete oxidation cycle (■). B) The corresponding CIE D65 color coordinates of the different device states in (A).

The increased absorbance is a result of the slightly thicker films of **3** used for the electrochromic device. In contrast, the color of the chemically oxidized **3** on substrates differed from the colors observed electrochemically in both devices and films. The color discrepancy between the chemically and electrochemically induced states is evident from the absorbance spectra in Figure 3A and 6A. The chemically induced absorbance was hypsochromically shifted by 110 nm relative to electrochemically induced absorbance change. The observed difference is in part owing to the different counter ions that are known to impact the color.[30] While the exact reason for the color difference cannot be unequivocally assigned, the collective chemical and electrochemical data nonetheless confirm that **3** can undergo both reversible and significant color changes upon oxidation. These data further confirm that **3** is a suitable electrochromic material in working devices.

The absorbance spectra of both the device (Figure 6A) and the electrochemically converted films (see the Supporting Information) had two absorbance peaks located at 365 and 690 nm in both their stable neutral and oxidized states. In the neutral state, the ratio of the 365/690 nm absorbance was greater than 3. The ratio decreased to less than 0.75 upon oxidation, resulting in a visible color change. The overall outcome is a large color change between the two states when the device is operated. Multiple switching between the two colored states was possible without significant color degradation. The performance of the patterned (*see* Supporting Information) and unpatterned electrochromic devices was examined by chronoamperometry under ambient conditions without device encapsulation. **Figure 7**A shows the transmission monitored at 690 nm, corresponding to the oxidized state, as a function of switching the device at +3.2 and −1.5 V bias at variable switching speeds. From the figure, it is clear that the device can be repeatedly switched between the two states. This is consistent with what was observed with the switching in acetonitrile with **3** immobilized on the ITO electrode. The highest change in transmission for the device between the neutral and oxidized states was 28% with 30 s switching speeds. The transmission ratio between the two states decreased inversely with switching speed, similar to what was also observed for the immobilized **3** in acetonitrile. This was a result of slow diffusion of the charge carrying electrolyte through the polymer film and not from degradation of the electrochromic layer. This is based on the observed consistent transmission difference between the two states where no noticeable decrease in the transmission was observed. The consistent transmission difference between the neutral and oxidized states further implies the robustness of **3** towards oxidative degradation in the electrochemically harsh device environment. While the duty cycle of **3** does not compare to that of devices prepared from other organic polymers, it should be placed in context that the device was operated under ambient conditions and it was not encapsulated. Typically, high duty cycles with organic electroactive layers are possible under anaerobic conditions and controlled environments such as device encapsulated that prevent the oxidative degradation of the electrochromic material. The moderate duty cycle of **3** under ambient conditions demonstrates the robustness of the polyazomethine towards decomposition by oxidation and hydrolysis in moist atmospheric environments. It is further noteworthy that this is the first successful example of a working electrochromic device using a polyazomethine as the electrochromic layer that exhibits a high color contrast between the neutral and charged states. Meanwhile, the consistent pattern between the spray-coated comonomers and the resulting on-substrate polymerized film of **3** serves of a proof-of-concept that the electrodes can readily be patterned with solution processsable comonomers via standard lithographic means without altering the pattern resolution.

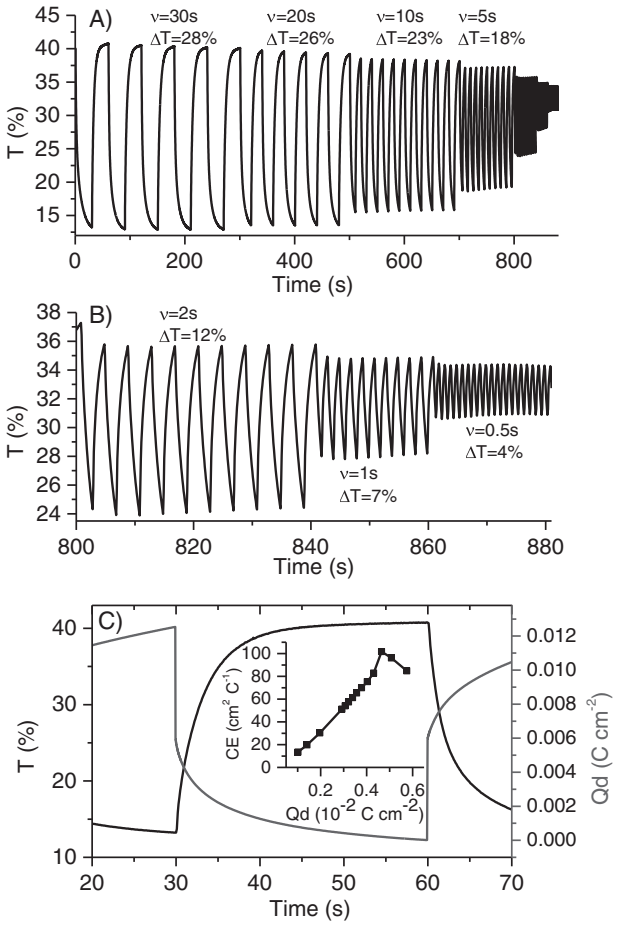

Figure 7. A) Transmittance of the electrochromic device of **3** monitored at 690 nm with applied voltages of 3.2 and −1.5 V at variable switching speeds. B) Magnified view of (A) at faster switching speeds. C) Transmittance at 690 nm (—) and charge density (—) of the transmissive electrochromic device of **3** as a function of time for one 30 s switch at 3.2 and −1.5 V. Inset: plot of coloration efficiency vs. charge density.

Figure 7C shows the transmittance and charge density as a function of cycle time. The coloration efficiency (η) of the device was derived from Figure 7C according to Equation 1, which takes into account the transmission% of the oxidized and neutral states and charge density. This leads to the coloration efficiency plot shown in the inset of Figure 7C and a maximum η of 102 cm^2 C^{-1} at 690 nm.

$$\eta = \frac{Log\left(\frac{T\%_{Neutral}}{T\%_{Oxidized}}\right)}{dQ} \quad (1)$$

3. Conclusion

In conclusion, the first example of an air-stable and moisture-resistant working electrochromic device successfully prepared from a conjugated polyazomethine was demonstrated. While the performance of the device may lag behind those prepared from other electroactive conjugated polymers, it nonetheless serves as a proof-of-concept that polyazomethines can successively be used as electrochromic materials. More importantly, the spectroelectrochemical studies confirmed that the immobilization of the polyazomethine could sustain an unprecedented moderate duty cycle of oxidation/neutralization switching without color fatigue or polymer decomposition. Optimization of the electrochromic layer thickness and other parameters such as the gel thickness and operating the device under anaerobic conditions will undoubtedly improve the device performance. Meanwhile, the polymerization of the robust polymer can be done directly on the working electrode by heating the comonomer coated substrate. This on-substrate polymerization method boasts the advantage that either commercially available or easily prepared monomers can be used for preparing stable electroactive polymers. This is in contrast to other immobilization strategies involving cleavable groups that require the judicious design of precursors prepared from multistep syntheses. The on-substrate method further is a straight forward means of preparing conjugated polymers immobilized directly on the device electrode without stringent reaction conditions, with minimal waste, few by-products, and a simple purification involving rinsing the substrate postpolymerization, while being amenable to standard patterning methods. The on-substrate polymerization is additionally advantageous because electroactive polymers having a wide range of colors are potentially possible by mixing and matching various complementary diamine and dialdehyde monomers such as thiophenes, pyrroles, furans, fluorenes and carbazoles. The method is also potentially applicable to large scale and high throughput processing methods such as roll-to-roll device fabrication, while being an environmentally friendly process, given that the main by-product produced during the polymerization is water.

4. Experimental Section

General Experimental Conditions: Reagents, reactants, and solvents were used as received unless otherwise stated. Anhydrous and deoxygenated solvents were obtained with an activated alumina column system. ^1H and ^{13}C NMR spectra were recorded at room temperature on a 400 MHz spectrometer. All the samples were dissolved in deuterated solvents and the spectra were referenced to the solvent line ($CDCl_3$: ^1H = 7.26 and ^{13}C = 77.0 ppm) relative to TMS. Absorbance measurements were done on a Varian Cary 500 UV-vis-NIR spectrometer. Electrochemical measurements were performed on a multi-channel BioLogic VSP potentiostat. Tetrabutyl ammonium hexafluorophosphate (0.1 M) in acetonitrile was used as the electrolyte. A saturated Ag/AgCl reference electrode was used for solution redox measurements. Ferrocene was added at the end of the measurements to serve as an internal reference for calibrating the measured oxidation potentials.[13]

Synthesis: The required monomer **1** (Scheme 1) was prepared according to known methods.[14]

4,4′-Diformyl triphenylamine (**2**). Phosphorus oxychloride (16.7 mL, 0.18 mol) was added dropwise to a stirred solution of DMF (13.1 mL, 0.18 mol) in dichloroethane (50 mL) at 0 °C. After the addition of triphenylamine (5 g, 0.02 mol) dissolved in dichloroethane (50 mL), the mixture was stirred at 90 °C for 12 h. After cooling, the solution was poured into cold water. The resulting mixture was adjusted to a neutral-basic pH with aqueous sodium hydroxide. The organic phase was then extracted with dichloromethane and it was washed twice with water (100 mL). The aqueous phase was also washed with dichloromethane

(100 mL). The organic fractions were combined and the solvent was removed under reduced pressure. The residue was purified by silica gel column chromatography (ethyl acetate/hexanes = 1/9) to afford the product as a yellow crystalline solid (4 g, 66%). Mp = 143 – 144 °C; ^{1}H NMR (400 MHz, $(CD_3)_2CO$, δ): 9.95 (s, 2H, CHO), 7.87 (Dt, J_D = 8.40 Hz, J_t = 2.03 Hz, 4H, Ar H), 7.49 (Tt, J_T = 8.25 Hz, J_t = 1.89 Hz, 2H, Ar H), 7.33 (Tt, J_T = 7.47 Hz, J_t = 1.20 Hz, 1H, Ar H), 7.25 (Tt, J_T = 8.39 Hz, J_t = 0.80 Hz, 4H, Ar H), 7.23 (s, 2H, Ar H); ^{13}C NMR (400 MHz $(CD_3)_2CO$, δ): 123.6, 127.1, 128.1, 131.1, 131.4, 132.6, 146.7, 152.9, 191.1; HRMS (ESI) m/z: calcd for $C_{20}H_{15}NO_2$, 301.2345; found, 302.1183.

Film Preparation: Monomer solutions of **1** and **2** were prepared in various concentrations and they were then sprayed onto 1.5 cm × 2 cm conductive glass substrates. Also, a mixture of the two monomers in a 1:1 stoichiometry was prepared in 1 mL of dichloromethane. The mixture was then sprayed evenly on the substrates with a spray gun at a distance of 10 cm using circular motions. The thickness of the resulting films could be adjusted between 50 and 400 nm by varying the concentration of the monomer solution.

Polymerization: The slides spray-coated with the two monomers were placed on a hot plate along with a small vial containing trifluoroacetic acid (TFA; 1 mL). A glass dish was then set on top to create a small chamber around the samples. The temperature was varied between 60 and 150 °C. Once a TFA saturated atmosphere was achieved, the slides were polymerized for between 15 and 45 min. After cooling, the substrates were washed with copious amounts of triethylamine that was diluted in dichloromethane followed by pure dichloromethane.

Electrochromic Device Fabrication: Transmissive devices were fabricated from films of **3** polymerized in situ on ITO glass electrodes. The device was prepared according to previously reported procedures with minor modifications to the gel electrolyte recipe.[5b,15] The electrolyte gel was prepared by combing propylene carbonate (PC), poly(ethylene glycol) diacrylate, and tetrabutyl ammonium tetrafluoroborate in the respective weight ratios of 10:7:3. 2,2-Dimethoxy-2-phenylacetophenone was used as the photoinitiator, which was added to the gel mixture in a 17.5 mg to 5 g ratio of PC.

A frame of double-sided adhesive foam tape was placed on a pristine 1.5 cm × 2 cm ITO-coated glass slide, leaving a half a centimeter border on one side. The gel electrolyte was deposited inside the frame with a Pasteur pipette. The polymer film coated ITO-glass slide was then placed on top of the gel coated ITO-glass and the device was placed in a UV chamber for photocuring the gel. The gel was cross-linked by irradiating it with three 350 nm lamps for 5 min. Copper tape was finally applied to both slides to serve as electrical contacts. The electrochemical properties of the device were measured with a potentiostat and the spectroscopic properties were measured with the above stated spectrometer.

Film Measurements: Film thickness measurements were done using the following method. The film was scored in three distinct places with a scalpel blade. Using a stylus profilometer, a 362 µm scan was performed over each scar. The thickness was determined from the average height of the three scans. Polymer films of **3** were prepared by spin-coating the required monomers onto glass microscope slides using the procedure above. The thickness and roughness of the polymer films were measured by tapping mode atomic force microscopy (AFM). The regions were scanned at 5, 10, and 25 µm resolutions using an amplitude setpoint of about 1 mV.

Supporting Information

Supporting Information is available from the Wiley Online Library or from the author.

Acknowledgements

L.S. and D.N. contributed equally to this work. NSERC Canada is thanked for Discovery, Strategic Research, Idea-to-Innovation, and Research Tools and Instruments grants allowing this work to be performed in addition to supplemental equipment funding from the Canada Foundation for Innovation. The Centre for Self-Assembled Chemical Structures is also acknowledged.

Received: December 11, 2012
Revised: January 5, 2013
Published online: February 18, 2013

[1] a) C. Wang, H. Dong, W. Hu, Y. Liu, D. Zhu, *Chem. Rev.* **2012**, *112*, 2208; b) Y. Li, *Acc. Chem. Res.* **2012**, *45*, 723l; c) F. S. Kim, G. Ren, S. A. Jenekhe, *Chem. Mater.* **2010**, *23*, 682; d) Z.-G. Zhang, J. Wang, *J. Mater. Chem.* **2012**, *22*.

[2] a) S. R. Neufeldt, M. S. Sanford, *Acc. Chem. Res.* **2012**, *45*, 936; b) H.-Q. Do, O. Daugulis, *J. Am. Chem. Soc.* **2011**, *133*, 13577; c) T. Yokozawa, A. Yokoyama, *Chem. Rev.* **2009**, *109*, 5595; d) J. Sakamoto, M. Rehahn, G. Wegner, A. D. Schlüter, *Macromol. Rapid Commun.* **2009**, *30*, 653.

[3] a) A. R. Murphy, J. M. J. Fréchet, P. Chang, J. Lee, V. Subramanian, *J. Am. Chem. Soc.* **2004**, *126*, 1596; b) J. Liu, E. N. Kadnikova, Y. Liu, M. D. McGehee, J. M. J. Fréchet, *J. Am. Chem. Soc.* **2004**, *126*, 9486; c) B. D. Reeves, E. Unur, N. Ananthakrishnan, J. R. Reynolds, *Macromolecules* **2007**, *40*, 5344; d) C. M. Amb, P. M. Beaujuge, J. R. Reynolds, *Adv. Mater.* **2010**, *22*, 724.

[4] a) Z. C. Smith, R. H. Pawle, S. W. Thomas, *ACS Macro Lett.* **2012**, 825; b) M. Helgesen, M. Bjerring, N. C. Nielsen, F. C. Krebs, *Chem. Mater.* **2010**, *22*, 5617; c) B. J. Kim, Y. Miyamoto, B. Ma, J. M. J. Fréchet, *Adv. Funct. Mater.* **2009**, *19*, 2273; d) S. Akimoto, D. Kato, M. Jikei, M.-a. Kakimoto, *J. Photopolym. Sci. Technol.* **1999**, *12*, 245; e) D. Burdi, S. Hoyt, T. P. Begley, *Tetrahedron Lett.* **1992**, *33*, 2133; f) A. L. Dyer, E. J. Thompson, J. R. Reynolds, *ACS Appl. Mater. Interaces* **2011**, *3*, 1787; g) J. G. Bokria, A. Kumar, V. Seshadri, A. Tran, G. A. Sotzing, *Adv. Mater.* **2008**, *20*, 1175.

[5] a) S. Alkan, C. A. Cutler, J. R. Reynolds, *Adv. Funct. Mater.* **2003**, *13*, 331; b) Y. Ding, M. A. Invernale, D. M. D. Mamangun, A. Kumar, G. A. Sotzing, *J. Mater. Chem.* **2011**, *21*, 11873.

[6] H. Meng, D. F. Perepichka, F. Wudl, *Angew. Chem., Int. Ed.* **2003**, *42*, 658.

[7] a) F.-C. Tsai, C.-C. Chang, C.-L. Liu, W.-C. Chen, S. A. Jenekhe, *Macromolecules* **2005**, *38*, 1958; b) C. L. Liu, W. C. Chen, *Macromol. Chem. Phys.* **2005**, *206*, 2212.

[8] a) A. Bolduc, C. Mallet, W. G. Skene, *Sci. China Chem.* **2013**, *56*, 3; b) S. Dufresne, W. G. Skene, *J. Phys. Org. Chem.* **2012**, *25*, 211.

[9] a) S. Dufresne, A. Bolduc, W. G. Skene, *J. Mater. Chem.* **2010**, *20*, 4861; b) A. Bolduc, S. Dufresne, W. G. Skene, *J. Mater. Chem.* **2012**, *22*, 5053.

[10] a) C. M. Amb, A. L. Dyer, J. R. Reynolds, *Chem. Mater.* **2010**, *23*, 397; b) P. M. Beaujuge, J. R. Reynolds, *Chem. Rev.* **2010**, *110*, 268; c) A. L. Dyer, M. R. Craig, J. E. Babiarz, K. Kiyak, J. R. Reynolds, *Macromolecules* **2010**, *43*, 4460; d) S. V. Vasilyeva, P. M. Beaujuge, S. Wang, J. E. Babiarz, V. W. Ballarotto, J. R. Reynolds, *ACS Appl. Mater. Interfaces* **2011**, *3*, 1022.

[11] T. Tshibaka, S. Bishop, I. U. Roche, S. Dufresne, W. D. Lubell, W. G. Skene, *Chem. Eur. J.* **2011**, *17*, 10879.

[12] a) S. Barik, T. Bletzacker, W. G. Skene, *Macromolecules* **2012**, *45*, 1165; b) F.-C. Tsai, C.-C. Chang, C.-L. Liu, W.-C. Chen, S. A. Jenekhe, *Macromolecules* **2005**, *38*, 1958; c) D. Sek, A. Iwan, B. Jarzabek, B. Kaczmarczyk, J. Kasperczyk, Z. Mazurak, M. Domanski, K. Karon, M. Lapkowski, *Macromolecules* **2008**, *41*, 6653.

[13] N. G. Connelly, W. E. Geiger, *Chem. Rev.* **1996**, *96*, 877.

[14] a) S. A. P. Guarìn, M. Bourgeaux, S. Dufresne, W. G. Skene, *J. Org. Chem.* **2007**, *72*, 2631; b) V. K. Gewald, M. Kleinert, B. Thiele, M. Hentschel, *J. Prakt. Chem.* **1972**, *314*, 303.

[15] a) M. A. Invernale, Y. Ding, D. M. D. Mamangun, M. S. Yavuz, G. A. Sotzing, *Adv. Mater.* **2010**, *22*, 1379; b) J. Kim, J. You, B. Kim, T. Park, E. Kim, *Adv. Mater.* **2011**, *23*, 4168.
[16] O. Thomas, O. Inganäs, M. R. Andersson, *Macromolecules* **1998**, *31*, 2676.
[17] a) D. S k, M. Lapkowski, H. Dudek, K. Karo , H. Janeczek, B. Jarz bek, *Synth. Met.* **2012**, *162*, 1046; b) D. Sek, M. Grucela-Zajac, M. Krompiec, H. Janeczek, E. Schab-Balcerzak, *Opt. Mater.* **2012**, *34*, 1333; c) A. Iwan, M. Palewicz, A. Chuchmała, L. Gorecki, A. Sikora, B. Mazurek, G. Pasciak, *Synth. Met.* **2012**, *162*, 143; d) J. C. Hindson, B. Ulgut, R. H. Friend, N. C. Greenham, B. Norder, A. Kotlewski, T. J. Dingemans, *J. Mater. Chem.* **2010**, *20*, 937.
[18] a) J. Cai, P. Zhao, H. Niu, Y. Lian, C. Wang, X. Bai, W. Wang, *Polym. Chem.* **2013**; b) L.-T. Huang, H.-J. Yen, J.-H. Wu, G.-S. Liou, *Org. Electron.* **2012**, *13*, 840; c) H. J. Yen, S. M. Guo, G. S. Liou, *J. Polym. Chem. A* **2010**, *48*, 5271; d) H. Y. Wu, K. L. Wang, J. C. Jiang, D. J. Liaw, K. R. Lee, J. Y. Lai, C. L. Chen, *J. Polym. Sci. A* **2010**, *48*, 3913; e) S.-H. Hsiao, G.-S. Liou, Y.-C. Kung, T.-J. Hsiung, *J. Polym. Chem. A* **2010**, *48*, 3392; f) G.-S. Liou, K.-H. Lin, *J. Polym. Chem. A* **2009**, *47*, 1988.
[19] H. R. Allcock, F. W. Lampe, *Contemporary Polymer Chemistry*, Prentice Hall, London **1990**.
[20] S. A. Pérez Guarìn, M. Bourgeaux, S. Dufresne, W. G. Skene, *J. Org. Chem.* **2007**, *72*, 2631.
[21] a) M. Bourgeaux, W. G. Skene, *Macromolecules* **2007**, *40*, 1792; b) S. Barik, W. G. Skene, *Macromolecules* **2010**, *43*, 10435; c) S. Barik, T. Bletzacker, W. G. Skene, *Macromolecules* **2012**, *45*, 1165.
[22] B. Lego, W. G. Skene, S. Giasson, *Macromolecules* **2010**, *43*, 4384.
[23] M. Bourgeaux, W. G. Skene, *J. Org. Chem.* **2007**, *72*, 8882.
[24] T. Skalski, Masters thesis, Université de Montréal, Montreal **2013**, 130.
[25] a) W. G. Skene, S. Dufresne, *Acta Cryst.* **2006**, *E62*, o1116; b) H. B. Bürgi, J. D. Dunitz, *Helv. Chim. Acta* **1970**, *53*, 1747; c) H. B. Bürgi, J. D. Dunitz, *Chem. Commun.* **1969**, 472; d) H. B. Bürgi, J. D. Dunitz, C. Züst, *Acta Cryst.* **1968**, *B24*.
[26] A. Bolduc, E. Knipping, W. G. Skene, *Acta Crystallogr., Sect. E* **2012**, *68*, o3262.
[27] C. B. Nielsen, A. Angerhofer, K. A. Abboud, J. R. Reynolds, *J. Am. Chem. Soc.* **2008**, *130*, 9734.
[28] A. J. Bard, L. R. Faulkner, *Electrochemical Methods: Fundamentals and Applications*, John Wiley & Sons, New York **2001**.
[29] J. Roncali, *Chem. Rev.* **1992**, *92*, 711.
[30] A. Bolduc, L. Rivier, S. Dufresne, W. G. Skene, *Mater. Chem. Phys.* **2012**, *132*, 722.